THE JOURNAL OF PHYSICAL CHEMISTRY C

Article

pubs.acs.org/JPCC

Controlled Mixed Violet–Blue–Red Electroluminescence from Eu:Nano-Phosphors/ZnO-Nanowires/*p*-GaN Light-Emitting Diodes

Oleg Lupan,*[,†,‡,§] Bruno Viana,*[,†] Thierry Pauporté,[‡] Maroua Dhaouadi,[†] Fabienne Pellé,[†] Lucie Devys,[∥] and Thierry Gacoin[∥]

[†]Laboratoire de Chimie de la Matière Condensée de Paris, UMR 7574-CNRS-ENSCP-UPMC, 11 rue P. et M. Curie, 75005 Paris, France

[‡]Laboratoire d'Electrochimie, Chimie des Interfaces et Modélisation pour l'Energie (LECIME), UMR 7575 CNRS, Chimie ParisTech, 11 rue P. et M. Curie, 75231 Paris cedex 05, France

[§]Department of Microelectronics and Semiconductor Devices, Technical University of Moldova, 168 Stefan cel Mare Blvd., Chisinau, MD-2004, Republic of Moldova

[∥]Laboratoire de Physique de la Matière Condensée, Ecole Polytechnique – CNRS, Route de Saclay , 91128 Palaiseau, France

ABSTRACT: Europium (Eu):Y_2O_3-nanoparticles/Mg:ZnO-nanowires/*p*-GaN and (Eu):chelate-based light-emitting diode (LED) structures have been fabricated, showing controlled mixed near-UV, violet, and red electroluminescence from trivalent europium. The magnesium (Mg)-doped ZnO (Mg:ZnO)-nanowires/*p*-GaN heterojunction were integrated into the LED structure and were covered on the top with the nanoparticle of yttrium oxide doped with trivalent europium ions (Eu^{3+}:Y_2O_3) or by Eu:chelate. Samples exhibit mixed UV/blue light at ~384 nm coming from the Mg:ZnO structure and a sharp red emission at ~611 nm related to the intra4f transition of Eu ions. It is found that with Mg doping of ZnO, the emission wavelength of LEDs in the near-ultraviolet region is shifted to a smaller wavelength, thus being better adapted to the trivalent europium excitation band. Radiative energy transfer is achieved through the strong overlap between the emission wavelength from *n*-(Mg:ZnO)/*p*-GaN heterojunction and $^7F_0$-$^5L_6$ absorption of Eu^{3+} ions in the case of Eu:Y_2O_3 or of the (Eu):chelate intensive absorption bands. Indeed, the (Eu):chelate/(Mg:ZnO)-nanowires/*p*-GaN structure appears to be more adapted to UV/blue and red dual emission than Eu:Y_2O_3, for which low absorption prevents efficient emission. Our results demonstrate that the designs of nano-LED structures and of the chelate ligands are crucial to enhance the performance of electroluminescence devices based on ZnO nanowire arrays and rare-earth metal complexes.

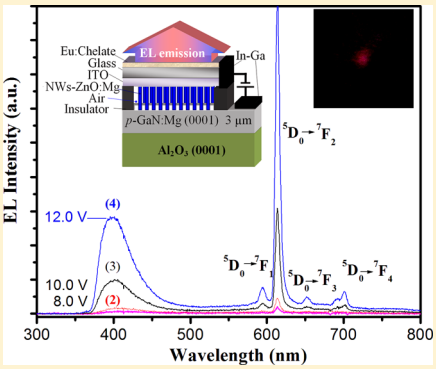

1. INTRODUCTION

Solid-state lighting devices are promising efficient lighting sources for displays and general illumination devices[1,2] owing to their lower energy consumption and longer lifetime compared with the incandescent bulbs. In recent years, there has been high interest and attention in systems based on europium (Eu) complexes and doped nano-ZnO for many promising photonic applications.[3−6] Among the different materials used as emitters in the light-emitting diodes (LEDs) design (as seen, for instance, in refs 6−8), europium complexes are attracting great attention because of their narrow (4f−4f) emission band in the red and their suitability for manufacturing pure red and full-color electroluminescent (EL) devices.[9−13]

Furthermore, considering the small oscillator strengths of the 4f−4f Eu^{3+} transitions, a sensitization process of the metal-ion luminescence has to be designed, involving energy transfer from coordinating species to the metal cation excited states. One way is to use energy-transfer paths through a long-lived ligand triplet state (T1).[12−16] It requires optimizing the energy gap between T1 and the emitting level of a lanthanide ion to obtain high sensitization efficiencies. Because triplet states are reached in the sensitization process,[13] one should expect the dominating contribution of triplet states in EL and an increase in the quantum efficiency (QE).[12] The figures of the external EL QE reported to date for Eu chelates-based LEDs are up to 4.5% photons/carrier.[15,17] It should, nevertheless, be noted that QE may be strongly reduced at larger current densities.[9,15,17,18]

Yttrium oxide doped with trivalent europium ions (Eu^{3+}:Y_2O_3) is a well known unsurpassed red-emitting phosphor used in: cathode ray tubes, fluorescent lamps and projection television tubes.[19,20] Moreover, it is a promising phosphor that can be developed at the nanoscale for field emission display devices.[21] Previous reported works demonstrate optical QE close to 95% for this phosphor;[22] therefore, this material seems well-suited for the new EL devices investigated in this paper. The Eu^{3+}:Y_2O_3 absorption feature

Received: August 4, 2013
Revised: November 8, 2013
Published: November 11, 2013

is constituted of narrow lines (related to Eu^{3+}) in the visible range, a broad band with a maximum at 250 nm related to the Eu^{3+}-O^{2-} charge transfer and strong absorption region below 230 nm due to the host lattice.[19] Both excitations of the host lattice and in the charge-transfer band lead to a strong emission in the red range at ~611 nm characteristic of the trivalent europium species.[19] The excitation mechanism of the phosphor is important because the trivalent europium cations cannot be directly and efficiently excited in its 4f bands due to the low oscillator strength of these transitions. In the present work, to use the phosphor in the LED system, ZnO/Eu^{3+} transfer is required to obtain strong red EL. It is the motivation of the present work to investigate and compare two possible systems, namely, Eu^{3+}-doped-Y_2O_3 nanoparticles and Eu:chelates. The effective overlap between the ZnO emission broad band and the absorption of the europium or host phosphor enable ultrafast energy transfer (ET) through a resonant radiative ET process, which is crucial for good efficiency. Direct ET from ZnO to Eu^{3+} has so far been quite low or even not observed.[23−30] In these works, defect states were involved in the ET process[26−30] because of the poor energy level overlap and due to the very short ZnO excitonic lifetime. This leads to poor ETs from ZnO to Eu^{3+} ions.[29] It has been proposed that the defect states in ZnO can temporarily store the excitation energy, which will then increase the efficiency of the ET from ZnO to Eu^{3+} ions.[29−31] Furthermore, radiative and nonradiative ETs have also been proposed in refs 26, 27, and 29−32.

In the present work, the introduction of Mg into the ZnO heterostructure has been done electrochemically and considered to tune the EL emission wavelength and adjust the emitted wavelength. The adjustment are in agreement with the phosphors optical characteristics and to enable an ultrafast and improved ET. In that case, red emission centered at ~611 nm could be observed when the samples were electrically excited by a 384 nm Mg:ZnO nanowire/*p*-GaN LED structure. In these heterostructures, the ET between the EL material and the europium-based phosphors was efficient due to the close distance between these two elements and the overlap of their optical features.[19,33]

Herein, we report on two different types of phosphor: Eu^{3+}-doped-Y_2O_3 nanoparticles and Eu:chelate, integrated in light-emitting device structures. The main goal of this work was to deposit phosphors as continuous layers on top of *n*-Mg:ZnO-nanowires/*p*-GaN, leading to the efficient Eu^{3+}:Y_2O_3/Mg:ZnO-nanowires/*p*-GaN and Eu:chelate/Mg:ZnO-nanowires/*p*-GaN heterostructures with controlled mixed blue/violet and blue/red emissions, respectively.

2. EXPERIMENTAL SECTION

The magnesium-doped ZnO nanowire arrays were grown by electrodeposition according to a procedure described elsewhere.[4,5,32,34−36] The substrate was a commercial magnesium-doped GaN (0001)-oriented single-crystal layer grown on sapphire with the *c* axis perpendicular to the substrate (purchased from TDI). The *p*-type GaN layer was 3 μm thick, and the dopant concentration was 3×10^{18} cm^{-3}. The crystal miscut was 0.59°. Magnesium chloride $MgCl_2$ (2.5 μM, 99.99% $MgCl_2 \cdot 2H_2O$, Aldrich) was used as the dopant in electrochemical bath for ZnO in the present work. Two trivalent based europium phosphors, Eu^{3+}-doped-Y_2O_3 nanoparticles and Eu:chelate, were tested in the present study.

Synthesis of the Eu:Y_2O_3 Nanoparticles. Eu^{3+}-doped yttrium oxide phosphors used in the study were an optimized commercial Eu^{3+}:Y_2O_3 product from General Electric (electronic phosphor reference GE-1281-274W) with particles size of ~50 nm and indicative light quantum yield of 95%.[21,37] Nanoparticles could also be prepared by various techniques to control their size in the nanoscale range.[37,38] In the literature, Eu^{3+}:Y_2O_3 nanoparticles have been prepared by a coprecipitation, sol−gel,[39] combustion methods,[40,41] which was also investigated, and other techniques.[42] In the present work, using a coprecipitation method, NH_4OH was added dropwise to a solution of europium nitrate dissolved in distilled water. The obtained hydrous gel was filtrated, washed with distilled water, and dried overnight. It was subsequently calcined at 1000 °C to obtain the pure phase. For the combustion method, also investigated, europium nitrate was dissolved in distilled water together with glycine in stoichiometric quantities. The mixture was dried overnight at 100 °C and then heated to 580 °C in an oven for 1.5 h. A white and very volatile powder was obtained after combustion. Part of this powder was further annealed at various temperatures up to 1400 °C to get the particle size variation. The nanoparticles were characterized by X-ray diffraction (XRD) using a Siemens D5000 diffractometer and the Cu Kα1 radiation with λ = 1.5406 Å. For transmission electron microscopy (TEM) measurements, nanopowders were ultrasonically dispersed in butanol, and a drop of solution was evaporated on a holey carbon copper grid. A high-resolution (0.19 nm) TOPCON OO2B operating at 200 kV was used to measure the TEM images of the nanoparticles. XRD patterns of the coprecipitation and combustion products indicate a pure Y_2O_3 cubic phase (the space group Ia3−) for any annealing temperatures (not shown here). Average particle size was estimated from XRD diffraction pattern using Scherrer formula. However, Scherrer formula yields the apparent or average particle size for a nanomaterial.

In the present work, a special attention was paid to the study of Eu:Y_2O_3 particles prepared by the combustion method, since this method has been less developed in the research literature. Figure 1a shows the XRD pattern recorded in the 20−70° range with a scanning step of 0.02° of Eu:Y_2O_3 particles. The pattern matches the lattice spacing of crystalline Eu:Y_2O_3 in the cubic phase (the space group Ia3-) and it is compared with a reference sample (Figure 1a). According to the TEM images shown in Figure 1b,c, the particle size depended on the annealing temperature. It was initially about 25 nm (Figure 1b) and it reached about 60 nm after thermal annealing at ~1100 °C and about 140 nm after thermal annealing at 1400 °C as presented Figure 1c. Then, in a second step, these nanoparticles dispersed in ethanol were deposited on the top of LED structure by using screen-printing technique.[39] These nanoparticles deposited as a film with thickness of 5−10 μm.

Synthesis of the Europium Chelate. A molecular phosphor $Eu(TTA)_3(H_2O)_3$, where TTA stands for thenoyltrifluoroacetone, was used for integration in LED structures. Our choice for the compound was governed by several arguments including: good solubility and simple synthesis, large absorption cross-section and good quantum yield, large Stokes shift between absorption and emission, absorption in the UV range compatible with LEDs and, as compared with dye molecules, good emission properties even in the bulk state. The Europium chelate was synthesized following the protocol described by De Silva et al.[43] First, 3 mM of potassium *tert*-butoxide was dissolved in 20 mL of water by heating at 60 °C in a round-bottomed flask under nitrogen atmosphere. Afterward, 3 mmol (mM) of the ligand TTA was progressively added. The mixture

dx.doi.org/10.1021/jp407783c | J. Phys. Chem. C 2013, 117, 26768−26775

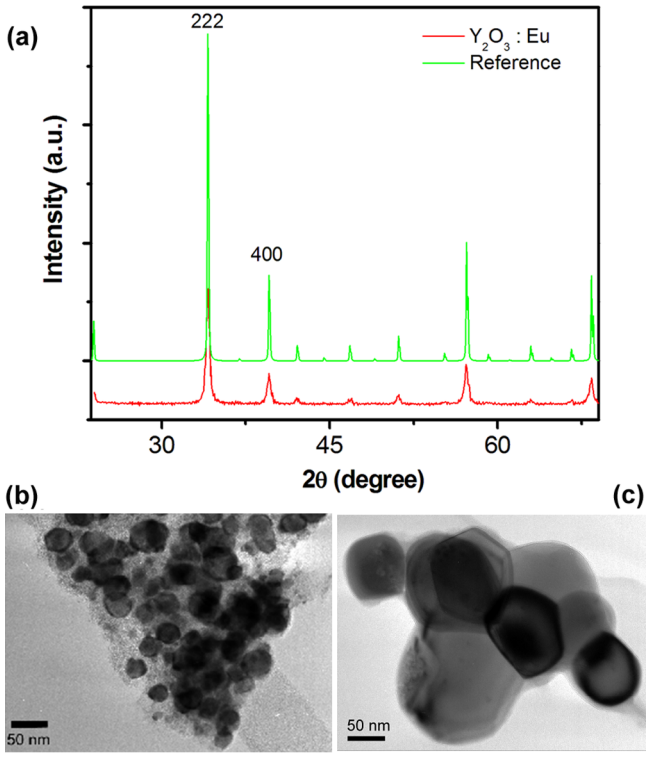

Figure 1. (a) XRD pattern of Eu:Y_2O_3-nanophosphors. TEM micrographs of Eu:Y_2O_3-nanophosphors obtained by combustion method: (b) without thermal treatment and (c) same as panel b after annealing at 1400 °C.

was stirred under nitrogen until complete dissolution (~30 min). An aqueous solution of Europium(III) chloride (1 mmol in 10 mL H_2O) was then added drop by drop under nitrogen. The solution became cloudy, and a white precipitate, luminescent under UV light, was formed. The mixture was heated at 60 °C during 30 min and then kept 3 h at room temperature under nitrogen and stirring. The precipitate was filtered and rinsed with a few milliliters of water and then with hexane. Finally, the obtained compound was dried one night under vacuum and used without any further purification. The complex had a quantum yield of 25% measured by comparison with calibrated standards. It presented a strong absorption cross-section in UV in the range of 350−400 nm, as detailed later.

Spray Deposition. The investigated europium chelate is highly soluble in ethanol and does not show significant extinction effect at high concentration or in the solid state. Therefore, it was not incorporated into a matrix. The molecule was simply dissolved in ethanol at 50 mg/mL, and the deposition was made by spray pyrolysis on the glass side of a manufactured microscope slide covered by indium−tin oxide (ITO). The setup is similar to the one used by Fleury et al.[44] To avoid any deterioration of the ITO film, we taped the substrate from the front side on the heated massive aluminum block. Afterward, 1 mL of the solution was deposited using a Paasche Talon gravity airbrush feed with a 0.38 mm nozzle. The air pressure was 1.5 atm, the air flow was ~100 mL/s, and the solution flow was ~0.1 mL/min. According to the literature,[43−45] heating the substrates at a temperature close to the evaporation temperature of the solvent appears to be the best deposition procedure to obtain spatially homogeneous films and avoid uncontrolled spreading of the solution. Thus, in our case, the ITO substrate was heated to 60 °C during the spray deposition.

Photoluminescence. Photoluminescence (PL) emission spectra were measured with a tunable optical parametric oscillator pumped with the third harmonic of a Nd:YAG Q-switched laser used as excitation source (Ekspla NT 342B-SH, 10 Hz repetition frequency, 6 ns pulse width). The luminescence was analyzed with a Jobin Yvon HR250 monochromator coupled to a Roper ICCD camera. With the ICCD camera, integrated and delay times were adjusted to the emission system. For Eu^{3+}, typical set-up was 5 ms (integration time) and 5 μs (delay time). Scanning electron microscopy (SEM) images were obtained by Hitachi S4800 FEG-SEM at 10 kV of accelerating voltage. The LED device structure assembly maintained by a bulldog binder clip was polarized with a Keitley 2400 source.[35] The EL was collected by an optical fiber connected to a CCD Roper Scientific detector (cooled Pixis 100 camera) coupled to a SpectraPro 2150i monochromator. The monochromator focal lens was 150 mm, and grating of 300 grooves/mm was blazed at 500 nm to record the emission over the whole ZnO-nanowires (NWs)/p-GaN near-UV−visible range. The CIE coordinates were calculated from this calibrated system.

3. RESULTS AND DISCUSSION

The integration of such phosphors onto the ZnO-NWs/*p*-GaN LEDs heterostructure was first investigated and is presented in the following part of the paper.

According to detailed cross-sectional SEM analysis of the edge of the evaporated Eu:chelate layer on glass (see Figure 2),

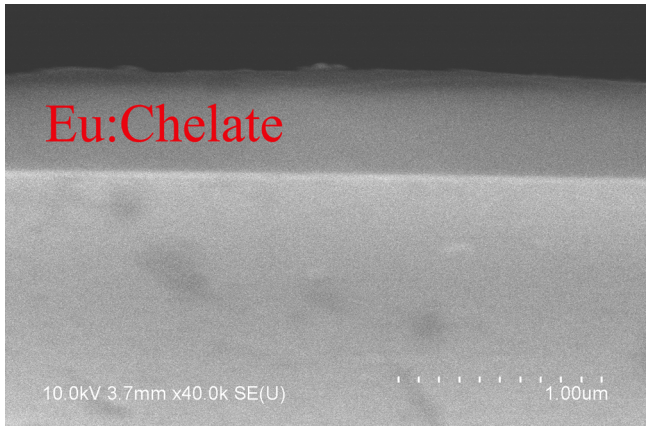

Figure 2. SEM image of the Eu:chelate/glass structure in cross-sectional view.

the thickness of Eu:complexes-chelate film was ~0.5 μm. SEM images demonstrated that the deposition was homogeneous on the substrate surface. Tang and VanSlyke[46] found that the morphological properties of the organic layers are critical in the construction of thin-film devices without pinholes. It is necessary that both layers in the EL device be smooth and continuous, as presented in Figure 2.

Magnesium-doped ZnO-NWs/*p*-GaN epitaxial heterojunction was used to construct a light-emitting diode structure, assembled as illustrated in the schematic of Figure 3, presenting the Y_2O_3:Eu^{3+}/Mg:ZnO-nanowires/*p*-GaN and Eu:chelate/Mg:ZnO-nanowires/*p*-GaN heterostructures-based LEDs. The top of the Mg:ZnO nanowire arrays was connected by ITO layer deposited on a transparent glass sheet/Eu:Chelate or

dx.doi.org/10.1021/jp407783c | J. Phys. Chem. C 2013, 117, 26768−26775

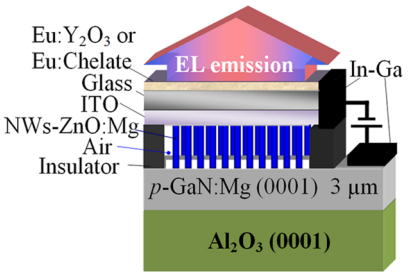

Figure 3. Schematic configuration (side view) of the Eu:Y_2O_3 or Eu:chelates/Mg:ZnO-nanowires/*p*-GaN LED structures.

Y_2O_3:Eu^{3+} nanoparticles. The top TCO (transparent conducting oxide) plate and the uncovered GaN layer were separated by a thin insulator[35] to avoid the direct contact between the two layers. The GaN layer was connected by In−Ga eutectic. More details of the fabrication of ZnO-nanowires/*p*-GaN LED structures can be found in refs 4, 5, and 35.

Figure 4 presents the excitation and emission spectra of the two phosphors. The excitation spectrum (Figure 4a, curve 1-blue) and the emission (Figure 4a, curve 2-red) have been reported for the commercial Eu^{3+}:Y_2O_3 nanocrystals with particle sizes of ∼50 nm (General Electric phosphor). The Eu^{3+}:Y_2O_3 sesquioxide phosphors with various sizes, elaborated by coprecipitation and combustion methods, presented the same optical features, but with lower emission efficiency than the commercial powder. Therefore they will not be further considered in this paper. The excitation band in Figure 4a extends between about 350 to 420 nm, with a characteristic structure coming from the 4f-4f absorption ($^7F_0$-$^5L_6$ manifolds transition). Such absorption ranging in the emission range of the ZnO-hybrid EL structure is associated with the low intensity of the 4*f*−4*f* Eu^{3+} transitions.[47−49] One can notice that the Eu−O charge-transfer band lies at a higher energy[19] and will not participate in the excitation process in the device. One can further notice that for Eu^{3+}:Y_2O_3 nanocrystals the features of the emission spectrum are similar to those of the bulk material reported in literature:[48] intense peak at 612 nm originates from $^5D_0 \rightarrow {}^7F_2$ forced electric-dipole transition of Eu^{3+}; the one centered at 633 nm corresponds to $^5D_0 \rightarrow {}^7F_3$ transition, and the peaks around 595 nm correspond to $^5D_0 \rightarrow {}^7F_1$ magnetic-dipole transition.[50] Small band peaking at 535 nm corresponds to $^5D_1$ emission.

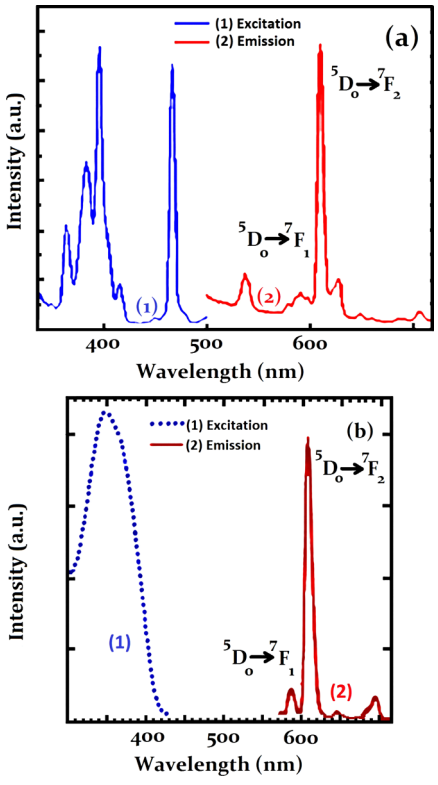

Figure 4. (a) Excitation and emission spectra of Eu^{3+}:Y_2O_3-nanocrystals with particle sizes of 50 nm, monitored for $^5D_0 \rightarrow {}^7F_2$ (611 nm emission) and 395 nm excitation, respectively. (b) Excitation spectrum (blue curve) of Eu:chelates when emission at 611 nm is monitored. Emission spectrum (red curve) of Eu:chelates (excitation wavelength 380 nm).

Figure 4b shows the excitation (curve 1-blue) and emission (curve 2-red) spectra of Eu:chelate samples under excitation wavelength of 380 nm. In these spectra, the intensity was normalized by the excitation intensity. The narrow emission peaks are assigned to $^5D_0 \rightarrow {}^7F_n$ (n = 0−4) transitions, with the strong emission at 612 nm originating from $^5D_0 \rightarrow {}^7F_2$ electronic dipole transition. Emission intensity of $Eu(TTA)_3(H_2O)_3$ is maximum when the complex is excited between 350 and 385 nm (curve 1, Figure 4b). These excitation wavelengths correspond to the absorption maxima of the *β*-diketonate ligands, confirming that the sensitization of the cationic metal center occurs efficiently by ET mediated by these ligands, consistent with the well-established mechanism of ligand-sensitized luminescence[43,46] of such hybrid phosphors. This absorption is indeed enhanced in regard to the forbidden 4f-4f rare earth absorption bands, which are not observed in the excitation spectrum.

Figure 5 shows the room-temperature EL spectra under a low forward bias voltage of 6.8 V for ZnO-NWs/*p*-GaN and Mg:ZnO-NWs/*p*-GaN LED structures. It can be seen that the structure based on Mg:ZnO demonstrates an enhanced EL intensity and an emission shifted toward shorter wavelengths (∼384 nm), which looks well-suited to the excitation band of the phosphors presented in Figure 4. As discussed by Li and coauthors,[51] the formation energy of zinc vacancies decreases with the increasing Mg content. This could be one of the reason for the increased efficiency observed in such LEDs. For

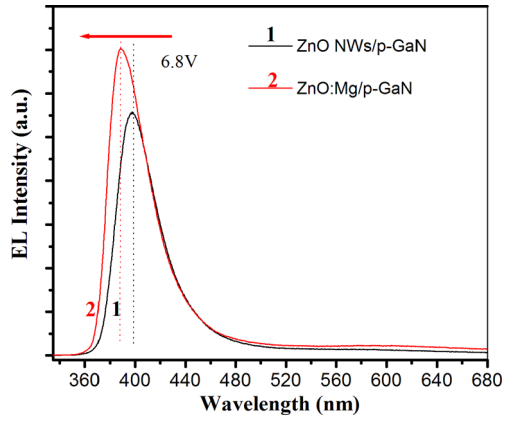

Figure 5. Room-temperature electroluminescence spectra of ITO/ZnO-nanowires/*p*-GaN and ITO/Mg:ZnO-nanowires/*p*-GaN LED structures (at 6.8 V).

dx.doi.org/10.1021/jp407783c | J. Phys. Chem. C 2013, 117, 26768−26775

further details of the characterization of the hybrid Mg:ZnO/GaN, please refer to ref 35. In the following study, only the optimized hybrid *n*-Mg:ZnO/*p*-GaN heterojunction has been used because its emission wavelengths are in better agreement with the phosphors' optical properties.

Figure 6 presents the room-temperature EL spectra of the Eu^{3+}:Y_2O_3/ITO/Mg:ZnO-nanowires/*p*-GaN LED structure (at

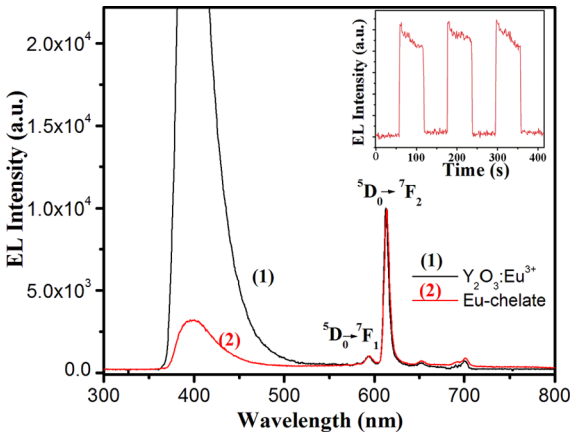

Figure 6. Room-temperature electroluminescence of the Eu^{3+}:Y_2O_3/ZnO:Mg-nanowires/*p*-GaN LED structure (at 8 V, curve 1) and of Eu:chelate/ITO/Mg:ZnO-nanowires/*p*-GaN LED structure (at 12 V, curve 2). Inset shows RT-EL time dependence under dc bias of 7 V for three switch-on/switch-off pulses (60 s between each one) for the Eu:chelate/ITO/Mg:ZnO nanowires/*p*-GaN LED structure. The emissions are normalized with the intensity of the $^5D_0 \rightarrow {}^7F_1$ (dipolar magnetic) transition.

8 V) and of Eu:chelate/ITO/Mg:ZnO-nanowires/*p*-GaN LED structure (at 12 V). They are characterized by intense emission peaks in both the UV and red wavelength ranges. The Eu:chelate/Mg:ZnO-NWs/*p*-GaN LED structure shows mixed near-band-edge EL peak of ZnO and sharp red luminescence originating from intra-4f shell Eu^{3+} $^5D_0 \rightarrow {}^7F_2$ transition. These results indicate that the luminescence occurs from both the LED and the Eu-based phosphors. It should be mentioned that the excitation wavelength (384 nm) for the EL measurement is indeed well-adapted to the absorption band of the Eu:chelate as presented in Figures 4b and 7, and Eu^{3+} chelate ligands present much stronger absorption than the direct Eu^{3+} 4f-4f absorption, as observed in the case of Eu^{3+}:Y_2O_3. Efficient emission at ∼611 nm is observed in Figure 6 in addition to the already reported Mg:ZnO emission at ∼384 nm.[4,5] This may open the door to realize the blue/red-light LEDs based on doped ZnO NWs. Comparison of two types of nanophosphors integrated in LEDs indeed shows that the Eu:chelate is more efficient in red emission than the Eu^{3+}:Y_2O_3 nanocrystals.

It is well known that direct ET from ZnO to Eu^{3+} ions is difficult to achieve when trivalent europium cations are inserted inside the ZnO structure due to the short lifetime of exciton in ZnO,[30,52] differences of ionic radii, and charges between Eu^{3+} and Zn^{2+} cations. Nevertheless, in the present work, the Mg:ZnO NW layer not only plays an important role in the emission wavelength tuning of ZnO NW but also could serve as a medium for radiative ET from Mg:ZnO to Eu^{3+} ions. A strong overlap between the emission from *n*-Mg:ZnO/*p*-GaN and ligands or $^7F_0$-$^5L_6$ absorption of Eu^{3+} ions is important for efficient and controlled red EL with such phosphors. Taking into account the bandgap of ZnO, the shallow level may be in line with the $^7F_0$-$^5L_6$ absorption band of Eu^{3+} ions (393 nm). Those defects located at the boundaries can serve as energy trap centers and support the transfer of energy in the system.[52] Kinetic experiments were performed to investigate the time response and the stability of the system. Figure 6(inset) illustrates the reproducibility of the response at the minimum voltage of 7 V for the Eu:chelate/*n*-Mg:ZnO/*p*-GaN hybrid structure. The same maximum of the emission was reached instantaneously (in <10 ms) after device switch-on, and the EL was immediately cut after the device switch-off. Many switch-on/switch-off cycles could be applied to the LED structure without any degradation of the performances or deterioration of the LED structure. Similar results (not shown) were obtained for the Eu^{3+}:Y_2O_3/Mg:ZnO-nanowires/*p*-GaN LED structure.

On the basis of the previous discussion, Figure 7a,b illustrates the excitation and emission processes that may occur for UV-excited Eu^{3+} doped phosphor emission. With Eu^{3+}:Y_2O_3/Mg:ZnO-nanowires/*p*-GaN LED structure, EL emission of the Mg:ZnO is generated due to the electron/hole recombination. The UV spectrum of the ZnO films strongly overlaps the absorption line of Eu^{3+} ions $^7F_0$-$^5L_6$. Hence, radiative ET from the Mg:ZnO emitter to Eu^{3+} ions takes place, promoting the Eu^{3+} ions from the ground-state $^7F_0$ to the excited-state $^5L_6$. The Eu^{3+} ions in the excited state $^5L_6$ undergo nonradiative

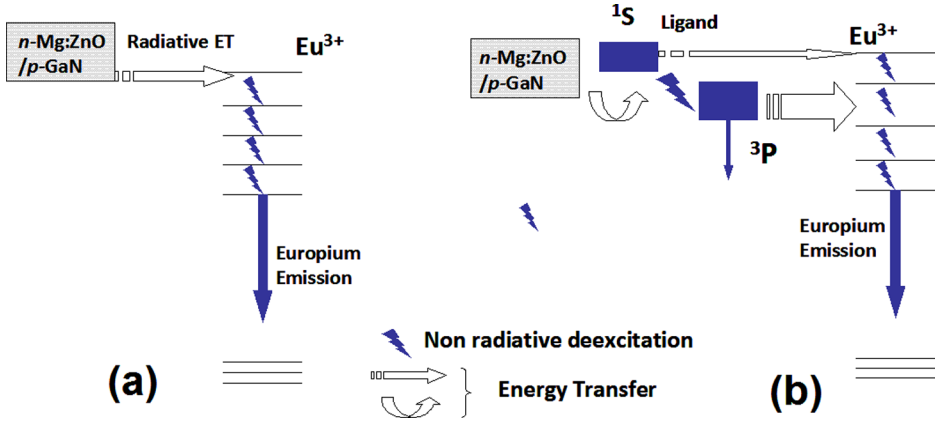

Figure 7. Simplified energy level diagram showing the main energy-transfer paths involved in the luminescence of Eu^{3+}-doped: (a) Y_2O_3 and (b) chelate systems. Arrows indicate emission and energy-transfer paths.

dx.doi.org/10.1021/jp407783c | J. Phys. Chem. C 2013, 117, 26768−26775

decay to the $^5D_0$ state because the gaps of adjacent levels are small. (See Figure 7.) Radiative transition takes place between the $^5D_0$ and the ^7F_J $J = 0-6$ states because of the larger gap.[20,53] The radiation is dominated by the red emission peak at ~611 nm, which arises from the $^5D_0$-$^7F_2$ transition. Because of the poor absorption strength of the 4f-4f transitions, the ET is limited. Additionally, the energy level of carriers trapped at the interface may also contribute to the mechanism. After relaxation, the excited carriers in Eu^{3+} ions recombine, also giving rise to $^5D_0$-^7F_J red emission.[52]

The NW-based LED structure could be favorable to the resonant ET. However, this is not the optimal case for the Eu:Y_2O_3 compound here because usually this phosphor is excited in the deep UV range at ~250 nm in the intensive O–Eu charge-transfer band.[19] The emissions resulting from the 384 nm transition and the 611 nm transition are shown in Figure 6.

The case of Eu:chelate/Mg:ZnO/GaN, as presented in Figure 7b, appears to be more favorable. The absorption of the chelate is more intense – allowed transition – and the ET could be enhanced, as presented in Figure 6, in the spectra normalized with the trivalent europium emission. The chelate-ligand energy levels could be drawn, being in good resonance (see Figure 4b) with the UV-LED emission. Again, nonradiative de-excitation occurs toward the $^5D_0$ emitting levels, and red emission is observed in these EL systems. These results show that there is an ET between the Mg:ZnO layers and Eu^{3+} ions, resulting in the red emission, which increases with the increasing overlap between the ZnO emission and ligand absorption.

Figure 8a presents the spectra characterized by the blue–red emission at different forward voltages applied to the nanoparticle-Eu^{3+}:Y_2O_3/Mg:ZnO-nanowires/*p*-GaN LED structures. The emission increased rapidly with the applied voltage and became intense above 8V (Figure 8a), proving that it is well-controlled by forward bias. Figure 8a (inset) shows an image of the violet–red light emission from Eu^{3+}:Y_2O_3/Mg:ZnO-nanowires/*p*-GaN LED system at 15 V forward bias, which can be clearly seen by the naked eye. Figure 8b shows the chromaticity coordinate diagram $X = 0.24$, $Y = 0.1$ for the Eu^{3+}:Y_2O_3/Mg:ZnO-nanowires/*p*-GaN LED system, indicating the violet color emitted by the LED. In that case, mainly the blue–violet LED emission was observed, as reported in the chromaticity coordinate diagram (Figure 8b).

Figure 9a presents room-temperature EL spectra of Eu:chelate/ITO/Mg:ZnO-nanowires/*p*-GaN LED structure for different applied forward voltages. It can be clearly observed that the blue emission peak centered at 384 nm and red emission peak centered at about 611 nm increased rapidly with the applied voltage and became intense above 8V (Figure 9a). These results demonstrate that developed LED structure is well-controlled by forward bias in a wide range. The inset shows red light emission from Eu:chelate/ITO/Mg:ZnO-nanowires/*p*-GaN LED at 8.5 V, which can be seen by the naked eye. Figure 9b displays the chromaticity coordinate diagram ($X = 0.40$, $Y = 0.25$) for the same structure. The chelate:Eu/Mg:ZnO-nanowires/*p*-GaN LED system presents a red emission in addition to the UV LED emission (Figure 9b). Figure 9a demonstrates the spectra of the blue–violet–red emission at four different forward voltages applied to the nanoparticle-Y_2O_3:Eu^{3+}/Mg:ZnO-nanowires/*p*-GaN LED structures, which can be controlled by external voltages. These experimental results prove that the proposed design of

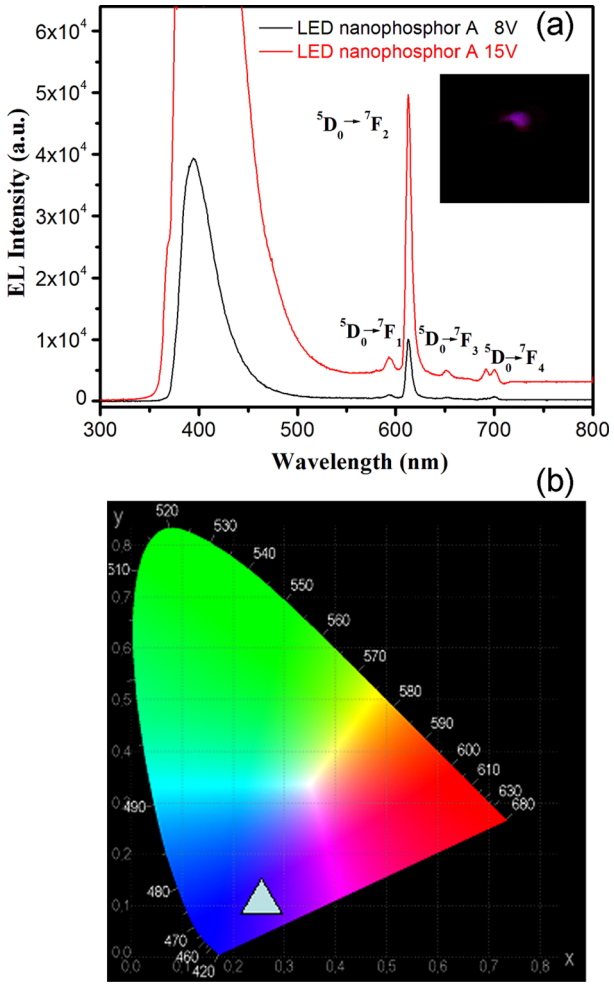

Figure 8. (a) Spectra of the red emission at two different forward voltages applied to the nanoparticle-Eu^{3+}:Y_2O_3/Mg:ZnO-nanowires/*p*-GaN LED structures. Inset shows a picture of the red light emission from LED at bias of 15 V. (b) Chromaticity coordinate diagram $X = 0.24$, $Y = 0.1$ for the Eu^{3+}:Y_2O_3/Mg:ZnO-nanowires/*p*-GaN LED system.

nanowire-based LEDs and of the nanophosphors are crucial to enhance the performance of mixed-color EL devices.

4. CONCLUSIONS

This work describes new designs for LEDs based on Eu-doped emitters and ZnO nanowire arrays showing dual visible UV-violet and red luminescence. We have studied their optical properties and have demonstrated that Eu:chelate/Mg:ZnO/*p*-GaN based-LED structures emit near-UV/blue light combined with red light at ~611 nm with good brightness. Samples exhibit sharp intense red emission related to the intra4f transition of Eu^{3+} ions. Comparison of two phosphors, Eu:Y_2O_3 and Eu:chelate was performed and discussed in terms of overlap between the emission from *n*-Mg:ZnO/*p*-GaN and Eu^{3+} or matrix energy levels. In addition, the directional guidance of emitted light from Mg:ZnO-nanowire/*p*-GaN heterojunction is favorable to enhance the phosphor absorption.[54−56]

It is found that with Mg doping in ZnO, the EL of LEDs is shifted toward the near-ultraviolet range, which favors red light emission from the phosphors while also decreasing the low wavelength component in the total output light. From the

dx.doi.org/10.1021/jp407783c | J. Phys. Chem. C 2013, 117, 26768−26775

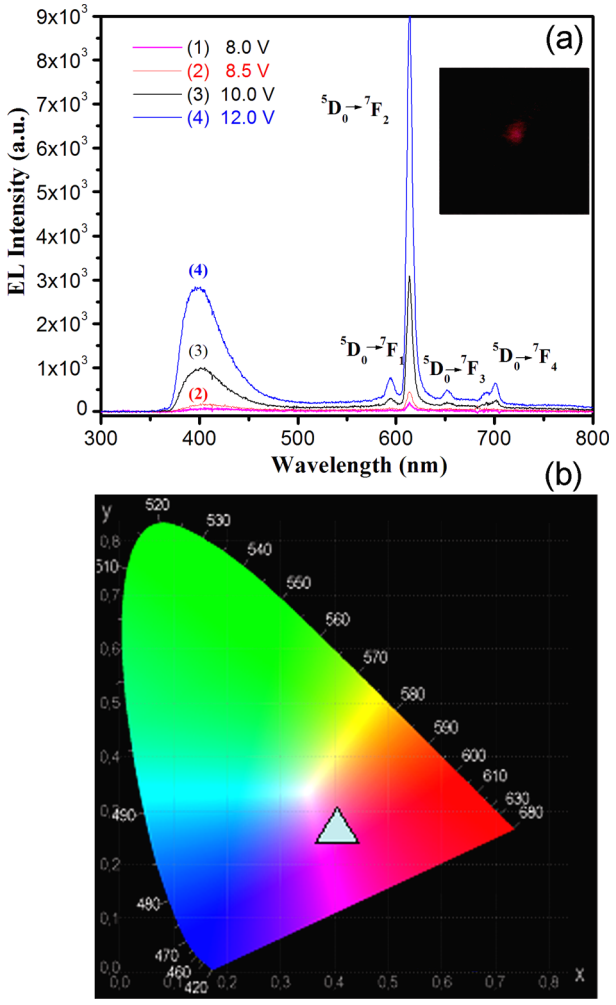

Figure 9. (a) Room-temperature electroluminescence spectra of Eu:chelate/ITO/Mg:ZnO-nanowires/*p*-GaN LED structure. Inset shows red light emission from LED at 8.5 V. (b) Chromaticity coordinate diagram $X = 0.40$, $Y = 0.25$ for the chelate:Eu^{3+}/Mg:ZnO-nanowires/*p*-GaN LED system.

results obtained with Eu:chelate/*n*-Mg:ZnO/*p*-GaN-based LED structures, future studies should be of interest, for example, by adding green emitting Tb^{3+} complexes on the way toward white hybrid LEDs.

Our results demonstrate that the designs of ligands and of nano-LED structures are crucial to enhance the performance of mixed-color EL devices based on doped ZnO NWs and rare-earth metal complexes. We showed that the UV emission spectrum of the ZnO can be tuned to strongly overlap with the absorption of Eu^{3+} ions by controlling the Mg doping. These results open the possibility to realize LEDs from lanthanide ions in nanowires devices based on radiative ET. Finally, our study provides a proof-of-concept that a magnesium-doped ZnO-NWs/*p*-GaN epitaxial heterostructure can be an efficient UV light excitation source for lanthanide-based emitting layers to design LED devices with tunable color emissions or mixed colors.

AUTHOR INFORMATION

Corresponding Authors

*Tel: (33)1 53 73 79 42. E-mail: oleg-lupan@chimie-paristech.fr.

*B.V.: bruno-viana@chimie-paristech.fr.

Notes

The authors declare no competing financial interest.

ACKNOWLEDGMENTS

Dr. Lupan acknowledges the CNRS for support as an invited scientist at the LCMCP-LECIME Chimie-ParisTech, ENSCP and the financial support of the STCU and ASM through grant 09_STCU_A/5833. Aschehoug P. (LCMCP, ENSCP, Paris) is acknowledged for PL measurements. This work has been partially supported by the C-nano Ile-de-France program (Effi-nanoLED Project).

REFERENCES

(1) *The Promise of Solid State Lighting for General Illumination: Light Emitting Diodes (LEDs) and Organic Light Emitting Diodes(O-LEDs)*; Optoelectronics Industry Development Association, U.S. Department of Energy: Washington, DC, 2001. http://lighting.sandia.gov/lightingdocs/OIDALEDOLEDSummary200103.pdf.

(2) Kim, T. H.; Wang, W.; Li, Q. Advancement in Materials for Energy-Saving Lighting Devices. *Front. Chem. Sci. Eng.* **2012**, *6* (1), 13−26.

(3) Chong, M. K.; Abiyasa, A. P.; Pita, K.; Yu, S. F. Visible Red Random Lasing in Y_2O_3:Eu^{3+}/ZnO Polycrystalline Thin Films by Energy Transfer from ZnO Films to Eu^{3+}. *Appl. Phys. Lett.* **2008**, *93*, 151105.

(4) Lupan, O.; Pauporté, T.; Le Bahers, T.; Viana, B.; Ciofini, I. Wavelength-Emission Tuning of ZnO Nanowire-Based Light-Emitting Diodes by Cu Doping: Experimental and Computational Insights. *Adv. Funct. Mater.* **2011**, *21*, 3564−3572.

(5) Lupan, O.; Pauporté, T.; Viana, B. Low-Voltage UV-Electroluminescence from ZnO-Nanowire Array/p-GaN Light-Emitting Diodes. *Adv. Mater.* **2010**, *22*, 3298.

(6) Lupan, O.; Pauporté, T.; Viana, B. Low-Temperature Growth of ZnO Nanowire Arrays on p-Silicon (111) for Visible-Light-Emitting Diode Fabrication. *J. Phys. Chem. C* **2010**, *114*, 14781−14785.

(7) Kalinowski, J. Electroluminescence in Organics. *J. Phys. D* **1999**, *32*, R179.

(8) Schubert, E. F. *Light-Emitting Diodes*; Cambridge University Press: New York, 2002; p 236.

(9) Jabbour, G. E.; Wang, J.-F.; Kippelen, B.; Peyghambarian, N. Sharp Red Organic Light-Emitting Devices with Enhanced Efficiency. *Jpn. J. Appl. Phys.* **1999**, *38*, L1553−L1555.

(10) Li, T.; Fukuyama, H.; Yamagata, Y.; Lan, H. L. Kido, Organic Electroluminescent Devices Using Europium Complex-Doped Poly(*N*-vinylcarbazole). *J. Polym. Adv. Technol.* **2004**, *15*, 302−305.

(11) Liu, H. G.; Lee, Y. I.; Park, S.; Jang, K.; Kim, S. S. Photoluminescent Behaviors of Several Kinds of Europium Ternary Complexes Doped in PMMA. *J. Lumin.* **2004**, *110*, 11−16.

(12) Kalinowski, J.; Stampor, W.; Cocchi, M.; Virgili, D.; Fattori, V. High-Electric-Field Quantum Yield Roll-Off in Efficient Europium Chelates-based Light-Emitting Diodes. *Appl. Phys. Lett.* **2005**, *86*, 241106.

(13) Bunzli, J. C. G.; Piguet, C. Taking Advantage of Luminescent Lanthanide Ions. *Chem. Soc. Rev.* **2005**, *34*, 1048−1077.

(14) Malta, O. L.; Brito, H. F.; Menezes, J. F. S.; Gonçalves e Silva, F. R.; de Mello Donegá, C.; Alves, S., Jr. Experimental and Theoretical Emission Quantum Yield in the Compound Eu(thenoyltrifluoroacetonate)$_3$.2(dibenzyl sulfoxide). *Chem. Phys. Lett.* **1998**, *282*, 233−238.

(15) Adachi, C.; Baldo, M. A.; Forrest, S. R. Electroluminescence Mechanisms in Organic Light Emitting Devices Employing a Europium Chelate Doped in a Wide Energy Gap Bipolar Conducting Host. *J. Appl. Phys.* **2000**, *87*, 8049.

(16) Kalinowski, J. *Organic Light Emitting Diodes: Principles, Characteristics, and Processes*; Marcel Dekker: New York, 2005; Chap. 1, Sec. 1.4.

(17) Hong, Z. R.; Liang, C. J.; Li, R. G.; Li, W. L.; Zhao, D.; Fan, D.; Wang, D. Y.; Chu, B.; Zang, F. X.; Hong, L. S.; et al. Rare Earth Complex as a High-Efficiency Emitter in an Electroluminescent Device. *Adv. Mater.* **2001**, *13*, 1241−1245.
(18) Baldo, M. A.; Adachi, C.; Forrest, S. R. Transient Analysis of Organic Electrophosphorescence. II. Transient Analysis of Triplet-Triplet Annihilation. *Phys. Rev. B* **2000**, *62*, 10967−10977.
(19) Blasse, G.; Grabmaier, B. C. *Luminescent Materials*; Springer: Berlin, 1994.
(20) *Phosphor Handbook*; Shionoya, S., Yen, W. M., Eds.; CRC: Boca Raton, FL, 1998.
(21) Bolchouchine, V. A.; Goldburt, E. T.; Levonovitch, B. N.; Litch-Manova, V. N.; Sochtine, N. P. Designed, Highly-Efficient FED Phosphors and Screens. *J. Lumin.* **2000**, *87*−*89*, 1277−1279.
(22) Ronda, C. R. Recent Achievements in Research on Phosphors for Lamps and Displays. *J. Lumin.* **1997**, *72*−*74*, 49−54.
(23) Ishizumi, A.; Taguchi, Y.; Yamamoto, A.; Kanemitsu, Y. Luminescence Properties of ZnO and Eu^{3+}-Doped ZnO Nanorods. *Thin Solid Films* **2005**, *486*, 50−52.
(24) Ishizumi, A.; Kanemitsu, Y. Structural and Luminescence Properties of Eu-doped ZnO Nanorods Fabricated by a Micro-emulsion Method. *Appl. Phys. Lett.* **2005**, *86*, 253106.
(25) Yang, C. C.; Cheng, S. Y.; Lee, H. Y.; Chen, S. Y. Effects of Phase Transformation on Photoluminescence Behavior of ZnO:Eu Prepared in Different Solvents. *Ceram. Int.* **2006**, *32*, 37−41.
(26) Bang, J.; Yang, H.; Holloway, P. H. Enhanced Luminescence of SiO_2:Eu^{3+} by Energy Transfer from ZnO Nanoparticles. *J. Chem. Phys.* **2005**, *123*, 084709.
(27) Yu, Y. L.; Wang, Y. S.; Chen, D. Q.; Huang, P.; Ma, E.; Bao, F. Enhanced Emissions of Eu^{3+} by Energy Transfer from ZnO Quantum Dots Embedded in SiO_2 Glass. *Nanotechnology* **2008**, *19*, 055711.
(28) Liu, Y.; Luo, W.; Li, R. F.; Liu, G. K.; Antonio, M. R.; Chen, X. Y. Optical Spectroscopy of Eu^{3+} Doped ZnO Nanocrystals. *J. Phys. Chem. C* **2008**, *112*, 686−694.
(29) Jia, W.; Monge, K.; Fernandez, F. Energy Transfer from the Host to Eu^{3+} in ZnO. *Opt. Mater.* **2003**, *23*, 27−32.
(30) Pauporté, T.; Pellé, F.; Viana, B.; Aschehoug, P. Luminescence of Nanostructured ZnO/Eu Mixed Films Prepared by Electro-deposition. *J. Phys. Chem. C* **2007**, *111*, 15427−15432.
(31) Wang, D.; Xing, G.; Gao, M.; Yang, L.; Yang, J.; Wu, T. Defects-Mediated Energy Transfer in Red-Light-Emitting Eu-doped ZnO Nanowire Arrays. *J. Phys. Chem. C* **2011**, *115*, 22729−22735.
(32) Lupan, O.; Pauporte, T.; Viana, B.; Aschehoug, P.; Ahmadi, M.; Roldan Cuenya, B.; Rudzevich, Y.; Lin, Y.; Chow, L. Eu-Doped ZnO Nanowire Arrays Grown by Electrodeposition. *Appl. Surf. Sci.* **2013**, *282*, 782−788.
(33) Chong, M. K.; Abiyasa, A. P.; Pita, K.; Yu, S. F. Visible Red Random Lasing in Y_2O_3:Eu^{3+}/ZnO Polycrystalline Thin Films by Energy Transfer from ZnO Films to Eu^{3+}. *Appl. Phys. Lett.* **2008**, *93*, 151105.
(34) Pauporté, T.; Lincot, D.; Viana, B.; Pellé, F. Toward Laser Emission of Epitaxial Nanorod Arrays of ZnO Grown by Electro-deposition. *Appl. Phys. Lett.* **2006**, *89*, 233112.
(35) Lupan, O.; Pauporté, T.; Viana, B.; Tiginyanu, I. M.; Ursaki, V. V.; Cortés, R. Epitaxial Electrodeposition of ZnO Nanowire Arrays on p-GaN for Efficient UV-Light-Emitting Diode Fabrication. *ACS Appl. Mater. Interfaces* **2010**, *2*, 2083−2090.
(36) Lupan, O.; Pauporte, T.; Viana, B.; Aschehoug, P. Electro-deposition of Cu-doped ZnO Nanowire Arrays and Heterojunction Formation with *p*-GaN for Color Tunable Light Emitting Diode Applications. *Electrochim. Acta* **2011**, *56*, 10543−10549.
(37) Justel, T.; Nikol, H.; Ronda, C. New Developments in the Field of Luminescent Materials for Lighting and Displays. *Angew. Chem., Int. Ed.* **1998**, *37*, 3084−3103.
(38) Williams, D. K.; Bihari, B.; Tissue, B. M.; McHale, J. M. Preparation and Fluorescence Spectroscopy of Bulk Monoclinic Eu^{3+}:Y_2O_3 and Comparison to Eu^{3+}:Y_2O_3 Nanocrystals. *J. Phys. Chem. B* **1998**, *102*, 916−920.
(39) Dhanaraj, J.; Jagannathan, R.; Kutty, T. R. N.; Lu, C. H. Photoluminescence Characteristics of Y_2O_3:Eu^{3+} Nanophosphors Prepared Using Sol−Gel Thermolysis. *J. Phys. Chem. B* **2001**, *105*, 11098−11105.
(40) Lee, M. H.; Oh, S. G.; Yi, S. C. Preparation of Eu-Doped Y_2O_3 Luminescent Nanoparticles in Nonionic Reverse Microemulsions. *J. Colloid Interface Sci.* **2000**, *226*, 65−70.
(41) Tessari, G.; Bettinelli, M.; Speghini, A.; Ajo, D.; Pozza, G.; Depero, L. E.; Allieri, B.; Sangaletti, L. Synthesis and Optical Properties of Nanosized Powders: Lanthanide-Doped Y_2O_3. *Appl. Surf. Sci.* **1999**, *144*−*145*, 686−689.
(42) Ye, T.; Guiwen, Z.; Weiping, Z.; Shangda, X. Combustion Synthesis and Photoluminescence of Nanocrystalline Y_2O_3:Eu Phosphors. *Mater. Res. Bull.* **1997**, *32*, 501−506.
(43) De Silva, C. R.; Maeyer, J. R.; Wang, R.; Nichol, G. S.; Zheng, Z. Adducts of Europium *β*-diketonates with Nitrogen *p*,*p*-Disubstituted Bipyridine and Phenanthroline Ligands: Synthesis, Structural Characterization, and Luminescence Studies. *Inorg. Chim. Acta* **2007**, *360*, 3543−3552.
(44) Fleury, B.; Dantelle, G.; Darbe, S.; Boilot, J. P.; Gacoin, T. Transparent Coatings Made from Spray Deposited Colloidal Suspensions. *Langmuir* **2012**, *28*, 7639−7645.
(45) Jiang, P.; McFarland, M. J. Large-Scale Fabrication of Wafer-Size Colloidal Crystals, Macroporous Polymers and Nanocomposites by Spincoating. *J. Am. Chem. Soc.* **2004**, *126*, 13778.
(46) Tang, C. W.; VanSlyke, S. A. Organic Electroluminescent Diodes. *Appl. Phys. Lett.* **1987**, *51*, 913.
(47) Weissman, S. I. Intramolecular Energy Transfer the Fluorescence of Complexes of Europium. *J. Chem. Phys.* **1942**, *10*, 214−217.
(48) Fu, Z.; Zhou, S.; Pan, T.; Zhang, S. Preparation and Luminescent Properties of Cubic Eu^{3+}:Y_2O_3 Nanocrystals and Comparison to Bulk Eu^{3+}:Y_2O_3. *J. Lumin.* **2007**, *124*, 213−216.
(49) Song, H.; Chen, B.; Peng, H.; Zhang, J. Light-Induced Change of Charge Transfer Band in Nanocrystalline Y_2O_3: Eu^{3+}. *Appl. Phys. Lett.* **2002**, *81*, 1776.
(50) Setua, S.; Menon, D.; Asok, A.; Nair, S.; Koyakutty, M. Folate Receptor Targeted, Rare-Earth Oxide Nanocrystals for bi-Modal Fluorescence and Magnetic Imaging of Cancer Cells. *Biomaterials* **2010**, *31*, 714−729.
(51) Li, Y.; Deng, R.; Yao, B.; Xing, G.; Wang, D.; Wu, T. Tuning Ferromagnetism in $Mg_xZn_{1-x}O$ Thin Films by Band Gap and Defect Engineering. *Appl. Phys. Lett.* **2010**, *97*, 102506.
(52) Chen, R.; Shen, Y. Q.; Xiao, F.; Liu, B.; Gurzadyan, G. G.; Dong, Z. L.; Sun, X. W.; Sun, H. D. Surface Eu-Treated ZnO Nanowires with Efficient Red Emission. *J. Phys. Chem. C.* **2010**, *114*, 18081−18084.
(53) Cotton, S. *Lanthanide and Actinide Chemistry*; Wiley: New York, 2006; Vol. *5*, pp 61−74.
(54) Lupan, O.; Pauporté, T. Hydrothermal treatment for the marked structural and optical quality improvement of ZnO nanowire arrays deposited on lightweight flexible substrates. *J. Cryst. Growth* **2010**, *312*, 2454−2458.
(55) Viana, B.; Lupan, O.; Pauporté, T. Directional and Magnetic Field Enhanced Emission of Cu-doped ZnO Nanowires/p-GaN Heterojunction Light Emitting Diodes. *J. Nanophotonics* **2011**, *5*, 051816.
(56) Lupan, O.; Pauporté, T.; Le Bahers, T.; Ciofini, I.; Viana, B. High Aspect Ratio Ternary $Zn_{1-x}Cd_xO$ Nanowires by Electro-deposition for Light-Emitting Diode Applications. *J. Phys. Chem. C.* **2011**, *115*, 14548−14558.